nature geoscience

LETTERS

PUBLISHED ONLINE: 5 FEBRUARY 2012 | DOI: 10.1038/NGEO1394

Underestimation of volcanic cooling in tree-ring-based reconstructions of hemispheric temperatures

Michael E. Mann[1]*, Jose D. Fuentes[1] and Scott Rutherford[2]

The largest eruption of a tropical volcano during the past millennium occurred in AD 1258–1259. Its estimated radiative forcing was several times larger than the 1991 Pinatubo eruption[1]. Radiative forcing of that magnitude is expected to result in a climate cooling of about 2 °C (refs 2–5). This effect, however, is largely absent from tree-ring reconstructions of temperature[6–8], and is muted in reconstructions that employ a mix of tree-rings and other proxy data[9,10]. This discrepancy has called into question the climate impact of the eruption[2,5,11]. Here we use a tree-growth model driven by simulated temperature variations to show that the discrepancy between expected and reconstructed temperatures is probably an artefact caused by a reduced sensitivity to cooling in trees that grow near the treeline. This effect is compounded by the secondary effects of chronological errors due to missing growth rings and volcanically induced alterations of diffuse light. We support this conclusion with an assessment of synthetic proxy records created using the simulated temperature variations. Our findings suggest that the evidence from tree rings is consistent with a substantial climate impact[2–5] of volcanic eruptions in past centuries that is greater than that estimated by tree-ring-based temperature reconstructions.

As with all climate proxies, tree-ring records have their own particular strengths and limitations. They are datable to the precise year, thus resolving specific events such as El Niño episodes or volcanic eruptions, and they often show a strikingly close relationship with climate variables. These relationships, however, typically hold only for the growing season[1,6–9]. Trees growing near the latitudinal or elevational treeline are typically selected for use in reconstructing past temperature changes[7,8] because their growth is primarily limited by temperature. One unintended consequence is that these same trees may not document the full extent of past cooling events, and in particular the response to the immense AD 1258/1259 eruption.

We employed simulations of the Northern Hemisphere mean temperature response to natural (volcanic+solar) and anthropogenic radiative forcing over the past millennium (Methods), using both a forced simulation[3] of the US National Center for Atmospheric Research (NCAR) CSM 1.4 coupled ocean–atmosphere general circulation model (GCM) and simulations of a simpler energy-balance climate model (EBM; refs 12,13). The EBM, though less comprehensive, is more amenable to extensive sensitivity analyses. Driven with estimated radiative forcings, both models capture the main features of the historical temperature record (Fig. 1a), including the abrupt multiyear cooling events following the major historical eruptions (the muted observed cooling following the Krakatau eruption of 1883 may be an artefact of data-quality issues in earlier decades[14]). Given their success in reproducing volcanic cooling events of the historical era, we might expect the models' predictions for previous centuries to be similarly reliable.

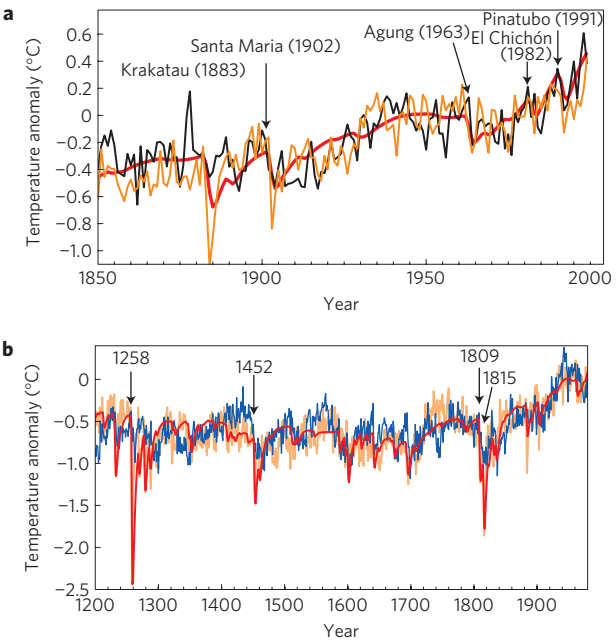

Figure 1 | Modelled Northern Hemisphere mean surface temperatures. EBM (red) versus GCM (orange) simulations. **a**, Modern Period, AD 1850–1999. Instrumental record[25] (black) shown for comparison. **b**, Pre-instrumental period, AD 1200–1980. The tree-ring record is shown for comparison (blue). Here and in all other figures, a 1961–1990 base period has been used for defining temperature anomalies. We confined this and similar later comparisons to the period AD 1200–1980 owing to a documented drop-off in statistical skill for the tree-ring reconstruction outside that interval[7].

Both models were driven with estimated forcings for the past millennium, during which several volcanic events dwarf any modern eruptions. The main features of the two simulations compare favourably (Fig. 1b). We then compared the simulations to a state-of-the-art tree-ring reconstruction of Northern Hemisphere temperatures based on a network of annual tree-ring thickness records from over 60 high-elevation and boreal treeline sites (consisting of 20 regional series) across North American and Eurasia[7].

Given the uncertainties in both the radiative-forcing estimates used to drive the climate models and the temperature reconstruction itself, the overall level of agreement is striking (Fig. 1b). Both simulations capture much of the low-frequency variation in

[1]Department of Meteorology and Earth and Environmental Systems Institute, Pennsylvania State University, University Park, Pennsylvania 16802, USA, [2]Department of Environmental Science, Roger Williams University, Bristol, Rhode Island 02809, USA. *e-mail: mann@psu.edu.

the reconstruction—and the residual variability (Supplementary Information) is within the estimated range of internally generated climate noise[13]. Yet there is one glaring inconsistency: the response to the three largest tropical eruptions—AD 1258/1259, AD 1452/1453, and the 1809+1815 double pulse of eruptions–is sharply reduced in the reconstruction. Both models predict a drop of ~2 °C following the 1258/1259 eruption, whereas the reconstruction shows a decrease of only ~0.6 °C. A similar pattern holds for the two other largest eruptions. Regardless of the predicted cooling, in no case does the reconstruction show more than −1.2 °C cooling relative to the modern base period; that is, there seems to be a ~1 °C floor on the cooling recorded by the reconstruction.

We first considered the hypothesis that the intrinsic noise of the tree-ring proxy data themselves might lead to an underestimation of the volcanic cooling signals in the reconstruction. Using the GCM simulation, we constructed a network of synthetic proxy records with the same hemispheric extent and signal-versus-noise properties as those estimated[7] for the underlying tree-ring data. Even the largest eruptions were difficult to discern in the individual synthetic proxy records because of the obscuring effects of both proxy noise and regional climatic noise (Supplementary Information). However, a simple hemispheric composite of the records, scaled to the target Northern Hemisphere mean-temperature series over the modern interval, yielded a faithful reconstruction with minimal underestimation of volcanic cooling (Fig. 2a). This familiar[15] result is a consequence of the cancellation of noise in a large-scale mean. Degradation by proxy noise consequently does not seem to represent a plausible explanation for the severe, preferential underestimation of the largest volcanic cooling events in tree-ring hemispheric temperature reconstructions.

We then explored the potential role of biological growth effects, using a model of tree growth appropriate for temperature-limited environments[16,17] (Methods). The daily growth model was driven by a climatological seasonal temperature cycle representative of typical treeline temperature conditions modulated by the simulated hemispheric temperature anomalies, to yield annual growth estimates. We also accounted for the influence of volcanic aerosol-induced increases in diffuse light on tree growth[18] (Methods). The resulting synthetic tree-growth series was scaled to the models' temperature series to yield a simulated 'tree-growth-based' temperature series.

The simulated series captures many of the features of the actual tree-ring temperature reconstruction, including the substantial underestimate of cooling for the largest eruptions and ~1 °C floor on cooling, whether derived from the GCM (Fig. 2b) or EBM (Fig. 2c) simulation. The GCM simulation is arguably more realistic as it includes the contribution of purely internal climate variability and, indeed, the tree-growth/temperature curve it generates shows a particularly good match to the actual series (Fig. 2b).

The same key features, however—that is, the greatly reduced simulated cooling following the major volcanic eruptions, including AD 1258/1259–are seen in both the GCM and EBM simulation. Using the EBM, moreover, we are able to establish that these findings are insensitive to (1) the precise climate sensitivity assumed, (2) the precise scaling assumed for past solar irradiance variations, (3) which of various alternative published volcanic aerosol-loading estimates[4,10,12] are used and (4) the scaling assumptions made to convert aerosol loading to volcanic forcing, that is, whether the radiative forcing is assumed linear with aerosol loading or instead follows a 2/3 power-law scaling to account for coagulation effects (reducing the impact of large eruptions[12]).

Stochastic daily temperature fluctuations can lead to non-zero growth even when the peak of the seasonal cycle lies below the threshold for growth T_{min}. To investigate the potential role of random weather forcing, we added Gaussian white noise

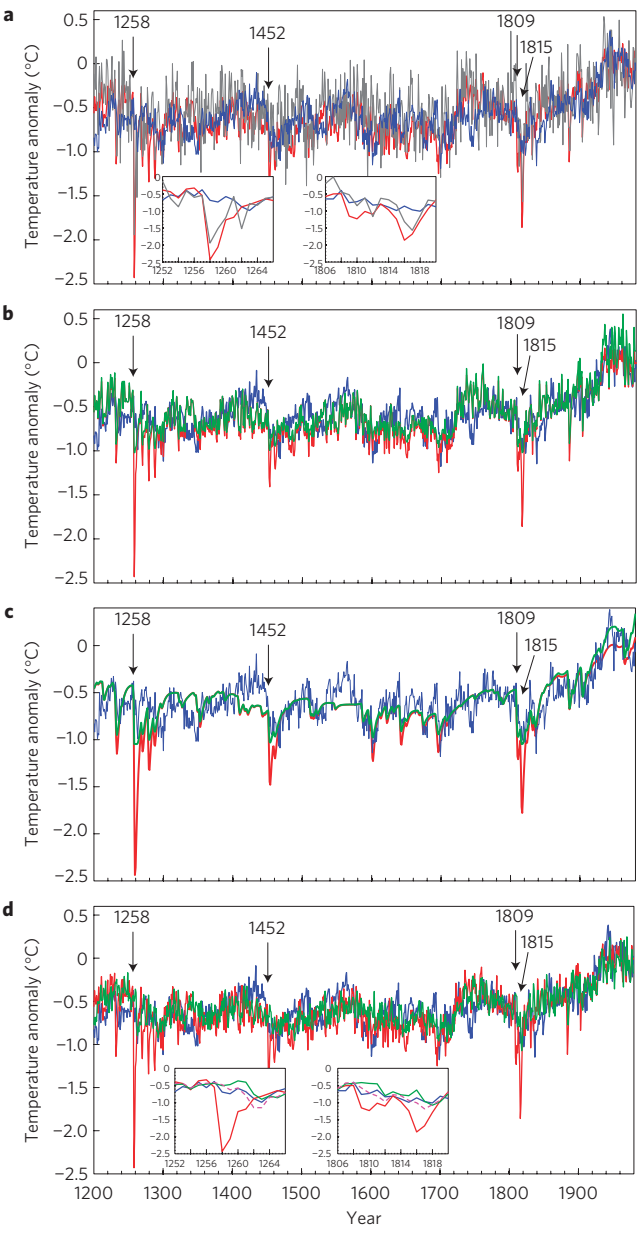

Figure 2 | Comparison of simulated and observed tree-ring reconstructions. a, GCM simulation (red), compared with composite-based 'pseudoproxy' reconstruction (the grey curve shows results for one particular random realization, but similar results are obtained for other realizations; see Supplementary Information) and actual (blue) tree-ring reconstruction. **b**, GCM simulation (red), compared with GCM-simulated (green) and actual (blue) tree-ring reconstructions. **c**, EBM simulation (red), compared with EBM-simulated (green) and actual (blue) tree-ring reconstructions. **d**, As in **a** but including the influence of stochastic weather forcing. Insets: Expanded views of the response to the AD 1258/1259 and AD 1809+1815 eruptions. The inset for **d** shows alternative results when the volcanic diffuse-light impact is ignored (dashed magenta).

with variance equal to that estimated for typical locations along the northern treeline to the simulated daily temperature series (Methods). We produced independent synthetic growth series for 20 'sites' to reflect the estimated synoptic-scale degrees of freedom sampled by the tree-ring network, with the mean over sites defining the hemispheric tree-growth series. The resulting series shows even better agreement (Fig. 2d) with the actual tree-ring reconstruction, providing a strikingly close reproduction of the observed behaviour

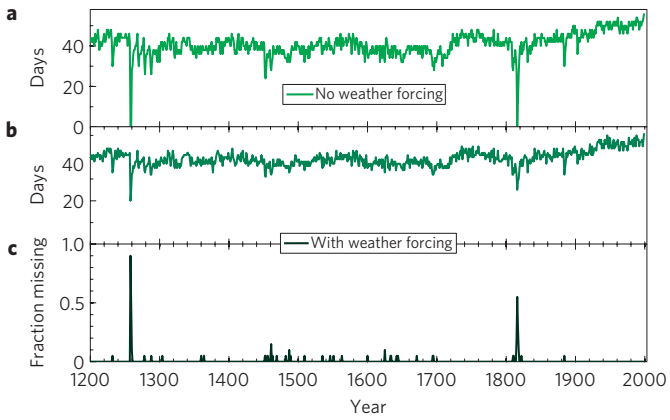

Figure 3 | Growing-season statistics. a,**b**, Estimated average length of the growing season (number of days of non-zero growth) based on the biological growth model driven by the GCM simulation without stochastic weather forcing (**a**) and with stochastic weather forcing (**b**). **c**, For the latter case, the fraction of the 20 regional series for which we infer a 'missing ring' for each year.

following the AD 1258/1259 and 1809+1815 eruptions, the reasons for which are discussed below.

Our findings are insensitive to the precise details of the growth model. The value $T_{min} = 10\,^{\circ}C$ for onset of growth is consistent with the published literature[19] and yields modern growing-season lengths (Fig. 3) most consistent with the documented range of 50–60 days at treeline[20]. Similar results are nonetheless obtained using for example a lower value $T_{min} = 7\,^{\circ}C$. Our results are also insensitive to the precise functional form[16,17] assumed for the growth function (Supplementary Information).

To better understand the role played by stochastic forcing, we must consider the potential impact of exceptionally short growing seasons on tree-ring age models. Following the volcanic eruptions of AD 1258 and 1809+1815, growing-season lengths fall to zero when stochastic forcing is not included (Fig. 3a); that is, there should be no growth and no 'ring' for that year. For each missing ring, an error of one year is introduced in the age model. For example, if there were no growth during 1816, then the 1815 growth ring would instead masquerade for the '1816' ring. Through this process, chronological errors will accumulate back in time as missing rings are encountered.

When stochastic forcing is included, there are fewer unusually short growing seasons on average (Fig. 3b). However, a large fraction (90%) of the 20 independent sites following the AD 1258/1259 eruption, and more than half of the sites following the 1815 eruption (Fig. 3c), have growing-season lengths that fall below a reasonably defined 'no-ring' threshold (we hypothesize that a ring may in practice not be discernible for growing seasons shorter than 26 days, but similar results are obtained assuming a shorter threshold, for example 14 days—Supplementary Information). The chronological errors accumulated from 'missing rings' necessarily differ among the various sites, each of which experiences different stochastic weather regimes. There is consequently increased temporal smearing back in time in the hemispheric composite. This smearing leads to a predicted delay of 1–2 years in the peak cooling for the 1815 eruption and an even larger delay of 4–5 years for the AD 1258/1259 eruption. It also leads to further reduction in the amplitude of the estimated cooling. These predicted features match quite closely with what is seen in the actual tree-ring series (Fig. 2d—see insets). The extent to which the predicted age-model errors are present in actual individual tree-ring series will need to be assessed by dendroclimatologists through the careful reanalysis of the original tree-ring data. It should also be noted that these age-model errors are predicted only for thermally limited treeline environments and for very large eruptions, and do not necessarily imply more general problems in dendrochronology.

Finally, let us consider the role that is played by the diffuse-light effect[2], which leads to a favourable growth response (that is, an apparent 'warming' tendency) in the first couple of years following the eruption. Although this effect is modest in our analyses (because trees–once they fall near or below the 'no-growth' threshold owing to prohibitively cool conditions–are unable to take advantage of any beneficial increases in diffuse light associated with volcanic eruptions), it is not negligible. It leads to a spurious apparent short-term warming that partly masks the volcanic cooling during the first couple of years, thus further reducing the amplitude of the recorded cooling, and shifting the peak apparent cooling forward in time. If this effect is not included, the match between the simulated and observed response to the AD 1258/1259 and 1809+1815 eruptions is not quite as good (Fig. 2d—see insets).

We have used a rather simple approach in this study. Logical extensions might account more explicitly for the regionally variable nature of the climate response to forcing, and use more elaborate tree-growth models. Yet our basic finding–that the damping and shifting of the expected cooling signature of major explosive volcanic eruptions in the tree-ring estimates of temperature over the past millennium is probably an artefact of the threshold-like behaviour of tree growth in a marginally favourable thermal environment—seems robust. In this sense, it provides a plausible and elegant hypothesis for explaining a heretofore vexing problem in paleoclimatology.

As tree-rings provide the only spatially extensive source of proxy climate information at annual resolution which span the past millennium, the potential biases identified in our study necessarily impact all existing hemispheric-scale estimates of the interannual cooling response to volcanic forcing in past centuries[10]. These biases might be alleviated by using alternative reconstruction approaches that model the underlying processes by which proxies record a climate signal[21], perhaps in conjunction with data-assimilation techniques[22]. Finally, our findings bolster the case for a significant influence of explosive volcanism on climate in past centuries, and are consistent with climate-model simulation results indicating that several explosive volcanic eruptions of the past millennium cooled the Earth by as much as 2 °C for several years at a time.

Methods

GCM simulation. We analysed the Northern Hemisphere mean (land+ocean) surface-temperature series from a simulation of the NCAR CSM 1.4 coupled GCM that was driven with estimated natural and anthropogenic forcing from AD 850 to 1999 (ref. 3). The natural forcing included estimated solar irradiance and stratospheric volcanic aerosols. Anthropogenic forcing included anthropogenic greenhouse gases and tropospheric aerosols. Further details are provided in Supplementary Information.

EBM simulations. We employed a simple zero-dimensional EBM (see for example refs 12,13) based on a linearized 'grey-body' approximation of outgoing long-wave radiation[23] with parameters chosen to yield a realistic pre-industrial global mean temperature ($T = 14.8\,^{\circ}C$) and an equilibrium climate sensitivity $\Delta T_{2xCO_2} = 3.0\,^{\circ}C$, consistent with mid-range Intergovernmental Panel on Climate Change estimates[24].

The model was driven with estimated annual mean natural and anthropogenic forcing over AD 850–1999 as taken from ref. 3. Further details are provided in Supplementary Information.

Sensitivity analyses were carried out with respect to (1) the equilibrium climate sensitivity assumed, (2) the solar scaling, (3) the volcanic aerosol loading estimates used and (4) the assumed scaling of volcanic radiative forcing with respect to aerosol loading to account for size-distribution effects. These alternative choices yielded qualitatively similar results (Supplementary Information).

Tree-growth model. We employed variants of the Vaganov–Shashkin tree-growth model[16,17]:

$$G(t) = g_E(t)\min[g_T(t), g_W(t)]$$

$g_E(t)$, $g_T(t)$ and $g_W(t)$ represent solar, thermal and moisture-dependent factors determining growth respectively. We approximated solar insolation as uniform

over the course of the short (<60 day) growing season at treeline. For thermally limited environments (that is boreal/alpine treeline), this yields

$$G(t) = g_E g_T(t)$$

$g_T(t)$ is taken[16,17] to have a functional dependence on daily mean temperature T characterized by an optimal growth range ($T_{opt1} < T < T_{opt2}$) and vanishing growth for low ($T < T_{min}$) or high ($T > T_{max}$) enough temperatures, through the piecewise continuous function (Supplementary Fig. S1a)

$$g_T(T) = \begin{cases} 0 & (T < T_{min}) \\ [(T - T_{min})/(T_{opt1} - T_{min})]^p & (T_{min} < T < T_{opt1}) \\ 1 & (T_{opt1} < T < T_{opt2}) \\ [(T_{max} - T)/(T_{max} - T_{opt2})]^p & (T_{opt2} < T < T_{max}) \\ 0 & (T > T_{max}) \end{cases}$$

$p = 1$ gives a trapezoidal response with linear side ramps[16,17], but quadratic side ramps ($p = 2$) are arguably more realistic. While we thus chose $p = 2$ as our default, similar results were obtained for $p = 1$ (Supplementary Fig. S11c). We adopted the ref. 17 values $T_{opt1} = 18\,^\circ$C, $T_{opt2} = 21\,^\circ$C and $T_{max} = 24\,^\circ$C. We favoured a value for T_{min} (10 °C) higher than the 5 °C value of ref. 17. While both values are consistent with the reported[19] range (5–10 °C), $T_{min} = 10\,^\circ$C gives more realistic[20] late-twentieth-century growing-season lengths at treeline (50–60 days; see Supplementary Fig. S12). Our overall findings are similar using lower values, for example $T_{min} = 7\,^\circ$C (Supplementary Fig. S11b), but with unrealistic growing season lengths of 80–90 days obtained (Supplementary Fig. S12).

The seasonal daily temperature cycle at treeline was modelled using

$$T_j = T_0(t) + T_2 + [(T_1 - T_2)/2][1 - \cos 2\pi(j/365)] + w(t)$$
$$(j = 1, \ldots, 365)$$

$T_0(t)$ is the annual hemispheric temperature anomaly (relative to the 1961–1990 baseline) for year t, and T_1 and T_2 are the maximum and minimum of the daily seasonal cycle respectively. We took $T_1 = 11.8\,^\circ$C, consistent with the 10–12.5 °C range for July mean temperature cited by ref. 19 (assuming a sinusoidal seasonal cycle, the mid-range value 11.25 °C implies a late-July peak temperature of $T_1 = 11.8\,^\circ$C). T_2 is more variable as it is not a primary control on treeline location, so we have simply taken a representative circumboreal treeline value $T_2 = -27\,^\circ$C (Supplementary Fig. S1b).

$w(t)$ represents stochastic weather forcing (assumed zero for no-noise simulations), and is defined by Gaussian white noise with daily standard deviation σ. Observational data for North American treeline locations suggests a representative growing-season (July–August) value of $\sigma = 3.0\,^\circ$C, but similar results are obtained (Supplementary Fig. S13) for modestly lower ($\sigma = 2.5\,^\circ$C) and higher ($\sigma = 3.5\,^\circ$C) values. Slightly different results are obtained for different weather-forcing realizations, but the main results shown in the article are robust to the particular noise realization.

An annual growth index $G_A(t)$ was defined as the sum of the daily $g(T_j)$ values over the course of year t. Growing-season length $L(t)$ was defined by the number of days of the year for which $g(T_j) > 0$.

The impact of increased diffuse radiation following volcanic eruptions was modelled by an extra term $D(t)$ in our expression for total tree growth:

$$G_T(t) = G_A(t)[1 + D(t)]$$

The impact of diffuse radiation on growth is assumed to scale linearly with aerosol optical depth, as per ref. 18, a roughly 30% increase in carbon assimilation for aerosol optical depths equivalent to 2 W m^{-2} radiative forcing, that is

$$D(t) = 0.3V(t)/2.0$$

$V(t)$ is the increase in diffuse radiation, roughly equal in magnitude to the decrease in direct radiation as per ref. 2. It is noteworthy that the diffuse-radiation effect alone, in the absence of a strong cooling-induced decrease in growth following large eruptions, yields unrealistic results (Supplementary Information).

Data and source code. Matlab code for the EBM and tree-growth model, all required data and results of the analyses are available at http://www.meteo.psu.edu/~mann/supplements/TreeVolcano12.

Received 14 June 2011; accepted 11 January 2012; published online 5 February 2012

References

1. Jones, P. D. & Mann, M. E. Climate over past millennia. *Rev. Geophys.* **42,** RG2002 (2004).
2. Robock, A. Cooling following large volcanic eruptions corrected for the effect of diffuse radiation on tree rings. *Geophys. Res. Lett.* **32,** L06702 (2005).
3. Ammann, C. M. *et al.* Solar influence on climate during the past millennium: Results from transient simulations with the NCAR Climate System Model. *Proc. Natl Acad. Sci.* **104,** 3713–3718 (2007).
4. Gao, C., Robock, A. & Ammann, C. Volcanic forcing of climate over the past 1500 years: An improved ice core-based index for climate models. *J. Geophys. Res.* **113,** D23111 (2008).
5. Timmreck, C. *et al.* Limited temperature response to the very large AD 1258 volcanic eruption. *Geophys. Res. Lett* **36,** L21708 (2009).
6. Esper, J., Cook, E. R. & Schweingruber, F. H. Low-frequency signals in long tree-ring chronologies for reconstructing past temperature variability. *Science* **295,** 2250–2253 (2002).
7. D'Arrigo, R., Wilson, R. & Jacoby, G. On the long-term context for late twentieth century warming. *J. Geophys. Res* **111,** D03103 (2006).
8. Briffa, K. R. *et al.* Trends in recent temperature and radial tree growth spanning 2000 years across northwest Eurasia. *Phil. Trans. R. Soc. B* **363,** 2269–2282 (2008).
9. Jansen, E. *et al.* in *IPCC Climate Change 2007: The Physical Science Basis* (eds Solomon, S. *et al.*) (Cambridge Univ. Press, 2007).
10. Mann, M. E. *et al.* Proxy-based reconstructions of hemispheric and global surface temperature variations over the past two millennia. *Proc. Natl Acad. Sci. USA* **105,** 13252–13257 (2008).
11. Salzer, M. W. & Hughes, M. K. Bristlecone pine tree rings and volcanic eruptions over the last 5,000 yr. *Quat. Res.* **67,** 57–68 (2007).
12. North, G. R., Cahalan, R. F. & Coakley, J. A. Energy balance climate models. *Rev. Geophys.* **19,** 91–121 (1981).
13. Crowley, T. J. Causes of climate change over the past 1000 years. *Science* **289,** 270–277 (2000).
14. Kennedy, J. J. *et al.* Reassessing biases and other uncertainties in sea-surface temperature observations since 1850 part 2: biases and homogenisation. *J. Geophys. Res* (in the press).
15. Mann, M. E. *et al.* Testing the fidelity of methods used in proxy-based reconstructions of past climate. *J. Clim.* **18,** 4097–4107 (2005).
16. Shashkin, A. V. & Vaganov, E. A. Simulation model of climatically determined variability of conifers' annual increment (on the example of common pine in the steppe zone). *Russ. J. Ecol* **24,** 275–280 (1993).
17. Evans, M. N. *et al.* A forward modeling approach to paleoclimatic interpretation of tree-ring data. *J Geophys. Res.* **111,** G03008 (2006).
18. Gu, L. *et al.* Response of a deciduous forest to the Mount Pinatubo eruption: Enhanced photosynthesis. *Science* **299,** 2035–2038 (2003).
19. MacDonald, G. M., Kremenetski, K. V. & Beilman, D. W. Climate change and the northern Russian treeline zone. *Phil. Trans. R. Soc. Lond. B* **363,** 2285–2299 (2008).
20. Rossi, S. *et al.* Evidence of threshold temperatures for xylogenesis in conifers at high altitudes. *Oecologia* **152,** 1–12 (2007).
21. Hughes, M. K. & Ammann, C. M. The future of the past—an earth system framework for high resolution paleoclimatology: Editorial essay. *Climatic Change* **94,** 247–259 (2009).
22. Goosse, H. *et al.* Using paleoclimate proxy-data to select optimal realisations in an ensemble of simulations of the climate of the past millennium. *Clim. Dynam.* **27,** 165–184 (2006.).
23. McGuffie, K. & Henderson-Sellers, A. *A Climate Modeling Primer* 2nd edn (Wiley, 1997).
24. IPCC *Climate Change 2007: The Physical Science Basis* (eds Solomon, S. et al.) (Cambridge Univ. Press, 2007).
25. Brohan, P. *et al.* Uncertainty estimates in regional and global observed temperature changes: a new dataset from 1850. *J. Geophys. Res.* **111,** D12106 (2006).

Acknowledgements

M.E.M. acknowledges support from the ATM program of the National Science Foundation (grant ATM-0902133). J.D.F. acknowledges support from the DOE (grant DE-FC02-06ER64298). We thank L. Ning and S. Miller for providing technical assistance.

Author contributions

M.E.M. carried out the modelling work. J.D.F. provided input on the biological modelling. S.R. assisted with the pseudoproxy tests. M.E.M. primarily wrote the paper. All three authors discussed results and provided input on the manuscript.

Additional information

The authors declare no competing financial interests. Supplementary information accompanies this paper on www.nature.com/naturegeoscience. Reprints and permissions information is available online at http://www.nature.com/reprints. Correspondence and requests for materials should be addressed to M.E.M.